A Combined MR-PET Analysis of Wholefield and Subfield Hippocampal Changes in AD and FTLD

Courtney A. Bishop [1,2], Giovanna Zamboni [1,3], Juergen Dukart [6,7], Karsten Mueller [7], Henryk Barthel [9], Osama Sabri [9], Matthias L. Schroeter [7,8,10,11], Jerome Declerck [5], Dorit Merhof [4], Mark Jenkinson [1]

[1] FMRIB, Nuffield Department of Clinical Neurosciences, University of Oxford, UK

[2] Imanova Ltd, Hammersmith Hospital, UK

[3] OPTIMA, Experimental Medicine Division of NDM, University of Oxford, UK

[4] Visual Computing Laboratory, University of Konstanz, Germany

[5] Siemens Molecular Imaging, Oxford, UK

[6] LREN, Department of Clinical Neurosciences, CHUV, University Lausanne, Switzerland

[7] Max-Planck-Institute for Human Cognitive and Brain Sciences, University of Leipzig, Germany

[8] Day Clinic of Cognitive Neurology, University of Leipzig, Germany

[9] Department of Nuclear Medicine, University of Leipzig, Germany

[10] Leipzig Research Center for Civilization Diseases, University of Leipzig, Germany

[11] German consortium for frontotemporal lobar degeneration

January 4, 2013

Abstract

Introduction: The pattern of wholefield hippocampal atrophy in Alzheimer's disease (AD) is relatively well established from MRI, but that of frontotemporal lobar degeneration (FTLD) is less known. FDG-PET findings for these neurodegenerative dementias are heterogeneous, and limited to the whole hippocampus, so the mechanism of local hippocampal dysfunction is unclear. It is also uncertain whether single- or multi-modality measures are more informative for maximal group discrimination and individual clinical diagnosis of dementia. We aim to address these queries and study limitations using 3 Tesla high-resolution T1-weighted MRI combined with FDG-PET data.

Methods: Using a newly-improved, fully-automated hippocampal segmentation tool for MRI data (termed FIRSTv3), we performed a subject-specific region-of-interest analysis of wholefield hippocampal atrophy and FDG metabolism in AD (N=21) and FTLD (N=10) compared to controls (N=13), including: (i) analysis of variance on wholefield measures; (ii) vertex analysis of variations in hippocampal size/shape; and (iii) linear discriminant analysis to investigate classification accuracies of single- and multi-modality hippocampal measures. Additionally, novel analysis of hippocampal subfield metabolism was performed using state-of-the-art

image processing (including partial volume correction of high-resolution PET data, and subfield atlas mapping to each subject's anatomically precise MR image).

Results: Both AD and FTLD displayed significant hippocampal atrophy (p= 0.010 and 0.005, respectively), but atrophy on the right side showed greater similarity than on the left (Figures 1 and 2). AD-associated atrophy mapped to lateral CA1 areas of the body and tail (bilaterally), lateral and dorsolateral CA1 areas of the hippocampal head (left side only), and the CA23 subfield, whilst the FTLD group displayed additional left-sided medial and posterior atrophy of the hippocampal body and tail. Significant wholefield hypometabolism was only found in FTLD (Figure 1), driven primarily by left-side dysfunction in the semantic dementia subtype. Interestingly, results suggest that combined MR+PET measures give better dementia versus non-dementia diagnoses (79.4% - 92.3% overall classification accuracy), but single-modality measures perform better for subsequent discrimination between dementias (Figure 3). Furthermore, findings support the hypothesis that in AD a compensatory mechanism maintains neuronal activity despite structural atrophy, and the left CA23 subfield might be the first place where severe atrophy overwhelms this mechanism (Figure 4).

Conclusion: These results support multi-modal image analysis for improved understanding and diagnosis of dementia, as well as providing novel insight into the possible regional vulnerability and compensatory mechanisms of the human hippocampus.

Acknowledgements: EPSRC and Imanova Ltd for funding; University of Leipzig for data.

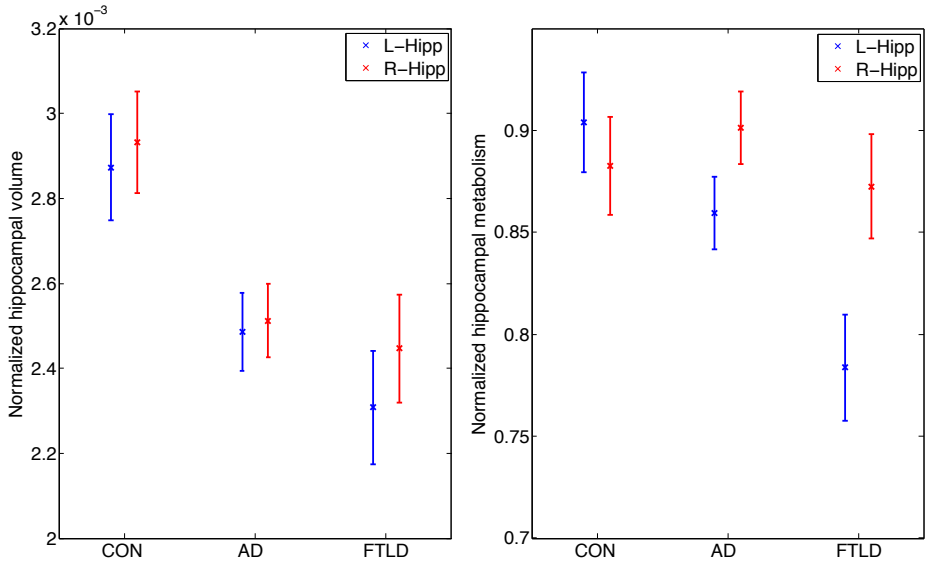

Figure 1. Estimated marginal means of normalized hippocampal volume (left plot) and normalized hippocampal metabolism (right plot) across group. Each pair of error bars show the standard errors for the left (left) and right (right) hippocampal measures. Volume is normalized by total intracranial volume (TIV), and metabolism is normalized by cerebellar FDG uptake.

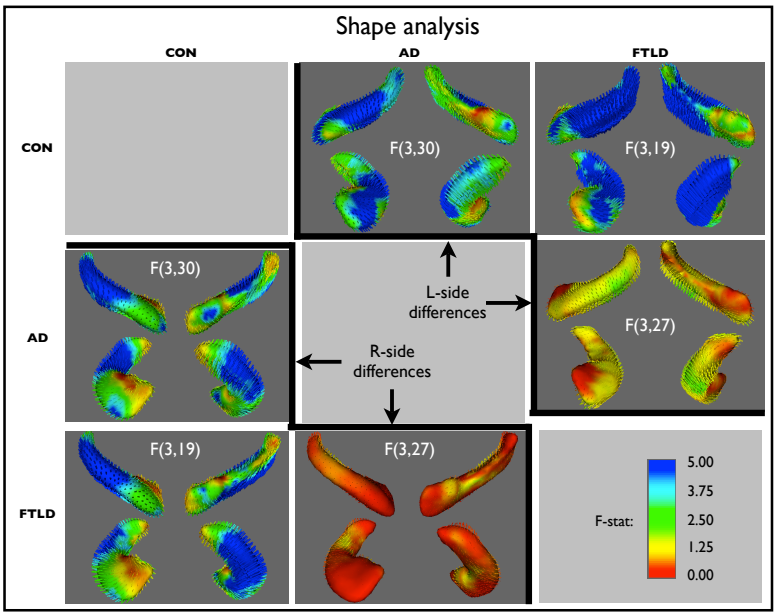

Figure 2. Vertex analysis results for group comparisons of hippocampal size/shape. Each 2x2 grid within a panel displays surface renderings for the lateral- (top left), medial- (top right), anterior- (bottom left) and posterior-view (bottom right). Surface colour gives the F-statistic for each group comparison, with blue indicating highly-significant group differences. Degrees of freedom (DOF) for each F-test are also given.

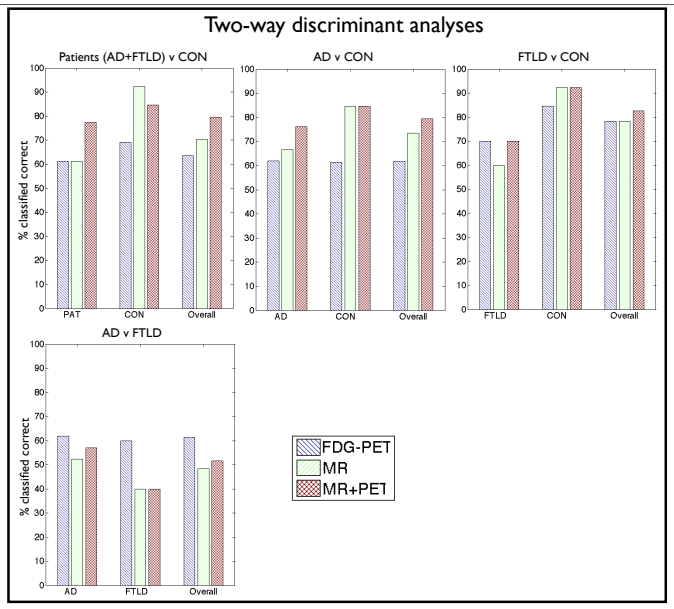

Figure 3. Percentage of cases (subjects) correctly classified using hippocampal FDG-PET metabolism (blue left-slanted lines, left bar of each triplet), MR volume (green right-slanted lines, middle bar of each triplet), and combined MR+PET measures (red criss-crossing lines, right bar of each triplet) as predictor variables in two-way linear discriminant analyses. For each plot, classification accuracy for each group (first and second triplet) is followed by the overall classification accuracy (third triplet).

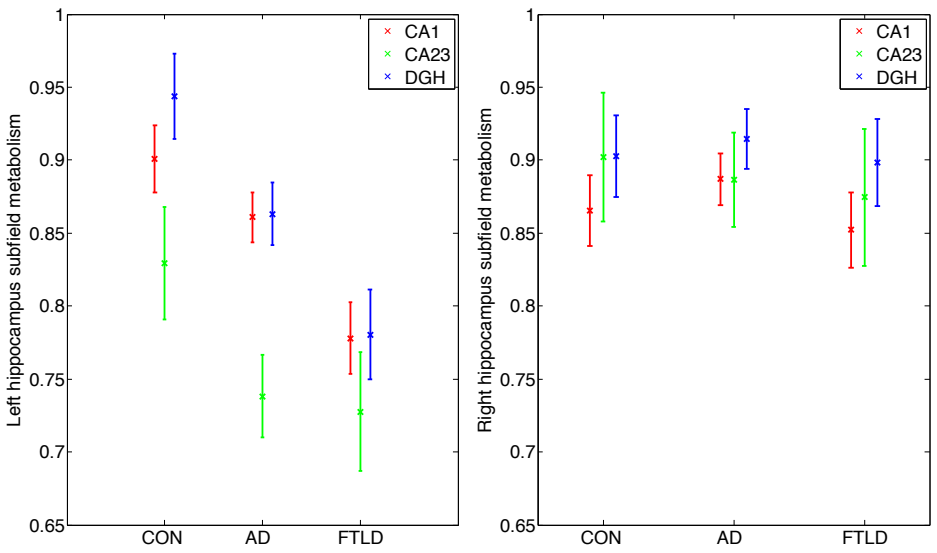

Figure 4. Estimated marginal means of left- (left panel) and right- (right panel) hippocampal subfield metabolism across group. Each triplet of error bars show the standard errors for the CA1 (left), CA23 (middle) and DGH (right) subfield. Metabolism is normalized by cerebellar FDG uptake.